Electronic-Structure Dependence of the Electron-Phonon Interaction in Ag

J. J. Paggel

Institut für Experimentalphysik, Freie Universität Berlin, 14195 Berlin, Germany

D.-A. Luh

Stanford Linear Accelerator Center, Menlo Park, California 94015, USA

T. Miller and T.-C. Chiang

Department of Physics, University of Illinois at Urbana-Champaign, Urbana, Illinois 61801-3080, USA
Frederick Seitz Materials Research Laboratory, University of Illinois at Urbana-Champaign, Urbana, Illinois 61801-2902, USA

The linewidths of sp- and d-band derived electronic quantum-well states in thin films of Ag on Fe(100) are measured as a function of temperature to yield the electron-phonon coupling parameters. The results vary by a factor of up to 35 among the different states. The origin of these huge differences is traced to the decay path selection for the various initial states of the holes created by the photoemission process. The electron-phonon coupling parameter for the top d-band quantum-well state, 0.015 ± 0.006, is the smallest ever reported.

Electron-phonon (e-ph) coupling plays a key role in many important and useful physical effects and phenomena, including superconductivity, charge density waves, and structural phase transitions [1]. Theoretical determination of this quantity is, however, difficult, and the results are often presented as an average over the Fermi surface to yield a momentum-independent parameter or Eliashberg function. Experimentally, it was only recently that angle-resolved photoemission emerged as a useful tool for this purpose [2], and it has since evolved rapidly into a widely used, albeit not completely understood, method. A basic implementation of the method is to measure the width of a photoemission peak as a function of sample temperature or, for states around the Fermi level, the deviation of the band dispersion from the noninteracting case [2–7]. The phonon-induced broadening or the electronic self-energy is then analyzed in terms of models with varying degrees of sophistication to yield a momentum-resolved, state-specific e-ph coupling parameter. Because of kinematic constraints of the photoemission process for three-dimensional systems, the width of a photoemission peak is often dominated by final-state lifetime broadening, which can make it very difficult to measure the true hole lifetime width [8,9]. For this reason, studies of e-ph coupling with angle-resolved photoemission have been mostly restricted to surface states or (quasi-) two-dimensional systems. For such cases, the experimental linewidth is a direct measure of the lifetime of the initial state. It is often quite small, thus allowing easy deduction of the small effect of e-ph coupling.

However, it is mostly the bulk states that are of interest and importance in regard to material properties relevant to applications. One approach to overcome the problem of final-state broadening for bulk states is to confine the bulk states in thin films. Confinement leads to the formation of quantum-well (QW) states which are two dimensional in nature [10,11]. As for surface states, there are no final-state contributions to the lifetime width of QW states, and the same methodology that has been highly effective for surface states can be employed. This method has been applied by at least two groups to study the effect of e-ph coupling in metallic QW systems [12–14]. Both groups reported an enhancement of the e-ph coupling parameter λ at small film thicknesses, but the interpretation is at variance in regard to whether this is a surface or interface effect. Nevertheless, both groups agree that the results converge to the bulk value at the thick-film limit. The convergence is governed by a $\sim 1/N$ dependence, where N is the film thickness in terms of monolayers.

In this Letter, we apply quantum-well spectroscopy as mentioned above to investigate e-ph coupling with a focus on an important issue that has thus far received relatively little attention. That is, the e-ph coupling parameter can depend on the specific state that is probed by angle-resolved photoemission, and we show that there can be very large differences between states of different angular momentum character or states at different binding energies. The systems under investigation are thin films of Ag on Fe(100), which can be prepared with atomic layer resolution, and QW states of both sp and d character have been reported [10,11,15]. In our work, we compare the e-ph coupling parameters for the sp and d states, and differences as large as a factor of 35 are observed. For the top QW peak derived from the d states, $\lambda = 0.015 \pm 0.006$, a value far smaller than any reported in the literature for a variety of systems, which are typically in the range of 0.1–1. This unusually small value is

explained in terms of available channels and phase space for hole decay governed by the band structure. The results generally illustrate the intricacy of e-ph coupling and the possible fallacy of working with average values.

All data presented here were taken with a goniometer-mounted electron analyzer with an angular resolution of ~1.5°, using monochromatic light from the U1-NIM undulator beam line of the Synchrotron Radiation Center, University of Wisconsin-Madison. Total energy resolution was set to 20 meV, as determined from spectra of the Ag Fermi edge. The Fe(100) substrate is a single-crystal whisker mounted on a liquid-nitrogen-cooled sample holder. The sample temperature was varied by direct current heating with a chopped power supply, and was measured by a thermocouple attached directly to the sample. Data acquisition took place in the off cycles of the sample heating current in order to avoid interference from the electric and magnetic fields generated by the current. The rate of Ag deposition was monitored with a quartz microbalance, and the final absolute thickness was determined by comparing the sp-band QW states to previous results calibrated by atomic layer counting [10,11].

Figures 1(a) and 1(b) show normal-emission spectra of the d-band and the sp-band regions, respectively, for a 10 monolayer (ML) thick Ag film. The spectra from the d-band region are characterized by two narrow QW peaks at binding energies of 3.74 and 3.84 eV, labeled 1 and 2, respectively, and broader d-band QW peaks at higher

binding energies. The influence of increasing temperature on the leading two peaks is very weak, and the thermal broadening is hardly visible to the eye. There is a slight change in the separation between the two peaks, which can probably be attributed to thermal expansion of the lattice [2,16]. The deeper d-band QW peaks show a much more obvious response toward increasing sample temperature, suggesting a significantly larger e-ph coupling parameter for these states. Our line shape analysis is restricted to the two leading peaks, as the rest of the d-band region contains the remaining 48 QW peaks, which are not resolved and therefore difficult to analyze. In contrast to the d-band peaks 1 and 2, thermal broadening of the sp-band QW peak is very pronounced, as seen in Fig. 1(b), again suggesting a significantly larger e-ph coupling parameter. This figure also displays the thermal broadening of the Fermi edge.

The sp- and d-band QW peaks are fitted as Voigt profiles with the Lorentzian contribution describing the lifetime and the Gaussian contribution accounting for the finite instrumental resolution of 20 meV. The resulting Lorentzian linewidths are displayed in Fig. 2. In the high temperature regime as is appropriate for the present experiment, the slope of a linear fit to the peak widths as a function of temperature is related to the e-ph coupling parameter λ [1]

$$\lambda = \frac{1}{2\pi k_B} \frac{d\Delta E}{dT}. \tag{1}$$

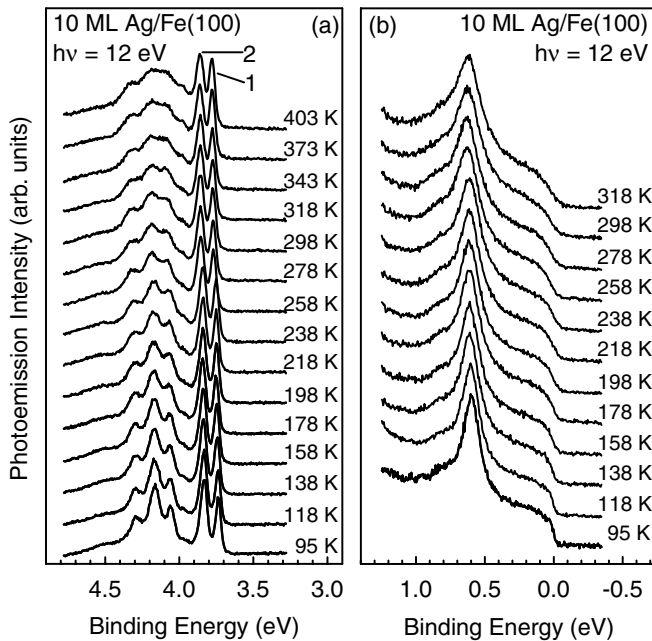Also shown in Fig. 2, for completeness, are the temperature-dependent shifts of the d-band QW peaks.

FIG. 1. Normal emission spectra taken with a photon energy of 12 eV and at various temperatures as indicated for a 10 ML Ag film on Fe(100) covering (a) the d-band region and (b) the sp-band region. A very weak peak at ~0.9 eV corresponds to a quantum well peak derived from a small admixture, at a few percent, of a 9-ML film thickness in the system; its intensity is accentuated by the photon energy chosen.
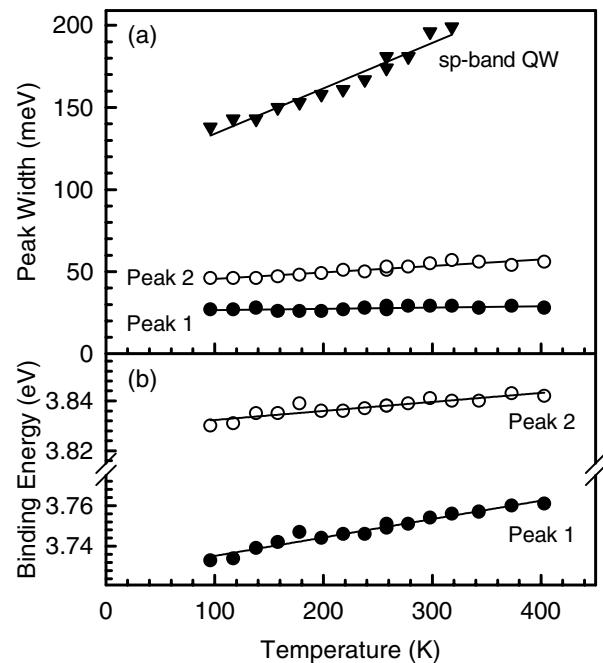

FIG. 2. (a) Lorentzian peak widths for d-band QW peaks 1 and 2 and the sp-band QW peak as a function of temperature. (b) Binding energies of d-band QW peaks 1 and 2 as a function of temperature. The straight lines are linear fits.

The values of λ derived for the d- and sp-band QW peaks are shown in Table I. The spread of the values is astounding. The smallest, $\lambda = 0.015 \pm 0.006$, comes from the top d-band peak. The next d-band QW peak gives $\lambda = 0.074 \pm 0.007$, which is about 5 times larger. λ for the sp-band QW peak, 0.52 ± 0.04, is still larger, being about 35 times as large as that from the top d-band QW peak. It is known that interface and surface effects influence the measurement of the e-ph coupling parameter in thin films [13,14]. For the sp state, the bulk limit of λ is about 0.29, and the measured value here at a film thickness of 10 ML is enhanced by interface effects. The d-band QW peaks, however, do not appear to be appreciably enhanced by any interface effects within our experimental error. Thus, the values of λ reported here for the d states should closely reflect the bulk limit.

TABLE I. Electron-phonon coupling parameters for the sp- and d-band quantum well states.

QW peak	λ
d band #1	0.015 ± 0.006
d band #2	0.074 ± 0.007
sp band	0.52 ± 0.04

Given the large differences among these numbers, it is clearly meaningless to quote a single e-ph coupling parameter. As the experiment shows, this parameter can depend sensitively on not only the angular momentum character of the states involved (sp vs d), but also the energy or momentum for a given character (peaks within the d manifold). A general expression for the inverse lifetime of a hole at $\vec{k}$ due to e-ph scattering is [1,6]

$$\frac{1}{\tau(\vec{k})} = \frac{2\pi}{\hbar} \sum_{\vec{k}',\vec{G},\vec{q},\eta} |g(\vec{k},\vec{k}',\eta)|^2 \times \left\{ \begin{array}{l} [f(E_{\vec{k}'}) + n(\vec{q},\eta)]\delta(E_{\vec{k}} - E_{\vec{k}'} + \hbar\omega(\vec{q},\eta))\delta_{\vec{k}+\vec{q},\vec{k}'+\vec{G}} \\ +[1 - f(E_{\vec{k}'}) + n(\vec{q},\eta)]\delta(E_{\vec{k}} - E_{\vec{k}'} - \hbar\omega(\vec{q},\eta))\delta_{\vec{k},\vec{k}'+\vec{q}+\vec{G}} \end{array} \right\}. \quad (2)$$

Here g is the matrix element describing the transition of an electron with momentum $\vec{k}'$ into a hole state with momentum $\vec{k}$, $\vec{G}$ is a reciprocal lattice vector, η is a phonon band index, $\vec{q}$ is the phonon wave vector, and ω is the phonon frequency. The two terms in the curly braces correspond to phonon absorption and emission, respectively, where f is the Fermi-Dirac distribution function for the electrons and n is the Bose-Einstein distribution for the phonons. Both the absorption and emission processes must conserve energy and momentum as required by the δ functions. Because of the boson nature of phonons, the absorption and emission processes are not symmetric, and phonon emission is always more probable based on the Bose statistics alone. At sufficiently high temperatures as is in the present experiment, the above expression can be simplified. The result is a linear dependence on T, and λ is proportional to the prefactor as in Eq. (1). The above discussion shows that λ is determined by available decay channels, available phase space for each decay channel, and the matrix elements for the scattering processes.

The hole states under consideration here are located at $\bar{\Gamma}$ by virtue of the normal-emission geometry. Schematic QW subband dispersions are illustrated in Fig. 3, and possible decay channels are sketched. Because phonon energies are much smaller than typical electronic energies, the range of k space involved is rather limited within the Brillouin zone, and the energy transfer in the e-ph scattering process is highly exaggerated in the diagram. The sp-QW subband is a free-electron-like parabola. Because it is convex, intraband decay processes at $\bar{\Gamma}$ are allowed for phonon emission only. Not shown here is the possibility of intersubband transitions, for which both phonon emission and absorption are allowed. Conversely, the dispersions of the d-band QW states are concave, and intraband decay of the hole at $\bar{\Gamma}$ can proceed via

phonon absorption only. For the top d-band QW state, this is the only possible decay channel, since the next d-band QW state lies about 100 meV below, which is larger than the maximum phonon energy. States that contribute to the decay of the top d-band QW state by phonon absorption are limited to a very small surface in the Brillouin zone as determined by energy and momentum conservation. For the next d-band QW state, the hole can decay through
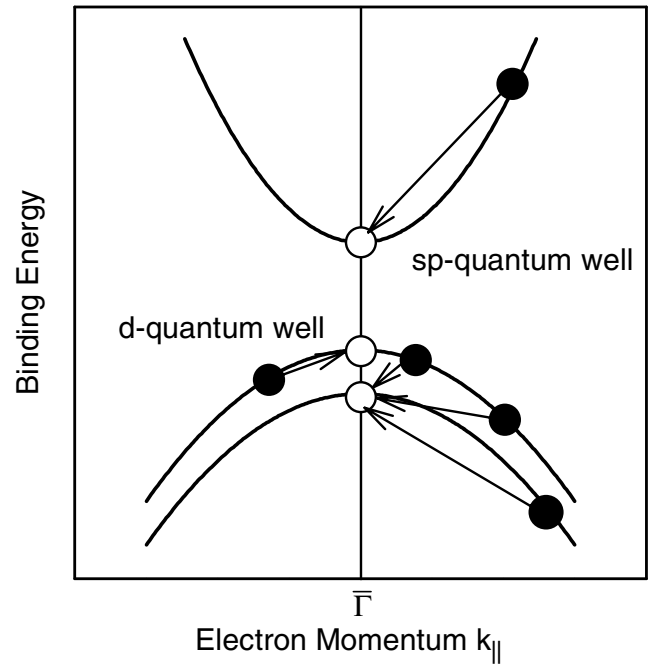

FIG. 3. Schematic illustration of the sp-band and d-band QW dispersion curves and hole relaxation paths. Hole states are indicated by open circles, while electrons are indicated by solid circles. The energy differences are highly exaggerated.

three channels: intraband phonon absorption as before and interband phonon absorption and emission. Compared to the top d-band QW state, a factor of 3 increase in λ, roughly, can be expected, as the matrix elements are expected to be similar. However, because of the energy offset between the two d subbands, the interband transitions actually encompass a larger surface on the top subband in the Brillouin zone (see Fig. 3). This increased phase space further enhances the scattering rate. An estimate based on the known band structure shows that this enhancement is roughly a factor of 2 for the interband channels. Considering both factors, our estimate is consistent with the observed ratio of ~ 5 in λ between the two d-band QW states. At still higher binding energies, the deeper d-band QW states have additional interband channels and even larger phase space for decay. Consequently, λ is expected to increase rapidly for increasing binding energies, as observed experimentally.

The argument in terms of available channels and phase space does not quite explain the huge difference between the d- and sp-QW states. Much of this difference can be related to the high degree of localization of the d states, resulting in a much smaller matrix element. Textbooks on solid state physics often invoke the rigid-ion approximation for formulating electron-phonon coupling [1]. The idea is that as atoms move by thermal vibration, their ionic cores modulate the electronic potential, which in turn causes electrons to scatter. The ionic cores are expected to be fairly rigid for thermal vibrations, and the rigid-ion approximation simply assumes that each ionic core is a rigid body. This is known to be an excellent approximation. The d states are fairly localized with characters resembling shallow core levels. They can be expected to move semirigidly with the ionic core and suffer much less scattering by thermal modulations of the potential. By contrast, the sp electrons are itinerant. They are not attached to any ionic core, and can be more easily scattered off by the potential modulation mostly in the interstitial region.

In conclusion, we have deduced the e-ph coupling parameter λ for various QW states in Ag via a temperature-dependent study. Several issues are addressed. One motivating issue is that the value of λ derived from quantum-well spectroscopy can be indicative of the true bulk value for sufficiently thick films. Our results show very large differences between states of different angular momentum character (sp vs d) and between states at different binding energies but of the same d character. Specifically, λ for the top d-band QW peak is far smaller than any reported in the literature. For the deeper d-band QW peaks, λ increases rapidly for increasing binding energies. The sp-band QW peak has a much larger λ than that for the top d-band QW peak. These results shed light on the basic physics of electron scattering by phonons. Three key factors are discussed: (1) available channels for scattering in terms of inter- and intraband transitions involving phonon emission and/or absorption; (2) phase space for each channel; and (3) matrix elements for the scattering process. The parameter λ plays an essential role in discussions of phase transitions. The large differences in λ observed here suggest that it is important to examine the interactions at the state-specific level.

[1] G. Grimvall, *The Electron-Phonon-Interaction in Metals* (North-Holland, Amsterdam, 1981).
[2] B. A. McDougall, T. Balasubramanian, and E. Jensen, Phys. Rev. B **51**, 13 891 (1995).
[3] M. Hengsberger *et al.*, Phys. Rev. Lett. **83**, 592 (1999).
[4] S. LaShell, E. Jensen, and T. Balasubramanian, Phys. Rev. B **61**, 2371 (2000).
[5] S. J. Tang, Ismail, P. T. Sprunger, and E. W. Plummer, Phys. Rev. B **65**, 235428 (2003).
[6] B. Hellsing *et al.*, Phys. Rev. B **61**, 2343 (2000).
[7] J. E. Gayone *et al.*, Phys. Rev. Lett. **91**, 127601 (2003).
[8] T.-C. Chiang, *et al.*, Phys. Rev. B **21**, 3513 (1980).
[9] N. V. Smith, P. Thiry, and Y. Petroff, Phys. Rev. B **47**, 15 476 (1993).
[10] J. J. Paggel, T. Miller, and T.-C. Chiang, Phys. Rev. Lett. **81**, 5632 (1998).
[11] J. J. Paggel, T. Miller, and T.-C. Chiang, Science **283**, 1709 (1999).
[12] J. J. Paggel, T. Miller, and T.-C. Chiang, Phys. Rev. Lett. **83**, 1415 (1999).
[13] D.-A. Luh *et al.*, Phys. Rev. Lett. **88**, 256802 (2002).
[14] M. Kralj *et al.*, Phys. Rev. B **64**, 085411 (2001).
[15] D.-A. Luh *et al.*, Phys. Rev. Lett. **84**, 3410 (2000).
[16] J. A. Knapp *et al.*, Phys. Rev. B **19**, 2844 (1979).